New Limits on Bosonic Dark Matter, Solar Axions, Pauli Exclusion Principle Violation, and Electron Decay from the Majorana Demonstrator

N. Abgrall *et al.* (Majorana Collaboration)

Phys. Rev. Lett. **118**, 161801 — Published 21 April 2017
DOI: 10.1103/PhysRevLett.118.161801

New limits on bosonic dark matter, solar axions, Pauli Exclusion Principle violation, and electron decay from the Majorana Demonstrator

N. Abgrall,[1] I.J. Arnquist,[2] F.T. Avignone III,[3,4] A.S. Barabash,[5] F.E. Bertrand,[4] A.W. Bradley,[1] V. Brudanin,[6] M. Busch,[7,8] M. Buuck,[9] T.S. Caldwell,[10,8] Y-D. Chan,[1] C.D. Christofferson,[11] P.-H. Chu,[12] C. Cuesta,[9] J.A. Detwiler,[9] C. Dunagan,[11] Yu. Efremenko,[13] H. Ejiri,[14] S.R. Elliott,[12] T. Gilliss,[10,8] G.K. Giovanetti,[16] J. Goett,[12] M.P. Green,[17,8,4] J. Gruszko,[9] I.S. Guinn,[9] V.E. Guiseppe,[3] C.R.S. Haufe,[10,8] R. Henning,[10,8] E.W. Hoppe,[2] S. Howard,[11] M.A. Howe,[10,8] B.R. Jasinski,[15] K.J. Keeter,[18] M.F. Kidd,[19] S.I. Konovalov,[5] R.T. Kouzes,[2] A.M. Lopez,[13] J. MacMullin,[10,8] R.D. Martin,[20] R. Massarczyk,[12] S.J. Meijer,[10,8] S. Mertens,[21,22] C. O'Shaughnessy,[10,8] A.W.P. Poon,[1] D.C. Radford,[4] J. Rager,[10,8] A.L. Reine,[10,8] K. Rielage,[12] R.G.H. Robertson,[9] B. Shanks,[10,8] M. Shirchenko,[6] A.M. Suriano,[11] D. Tedeschi,[3] J.E. Trimble,[10,8] R.L. Varner,[4] S. Vasilyev,[6] K. Vetter,[1,*] K. Vorren,[10,8,†] B.R. White,[12] J.F. Wilkerson,[10,8,4] C. Wiseman,[3] W. Xu,[15] E. Yakushev,[6] C.-H. Yu,[4] V. Yumatov,[5] I. Zhitnikov,[6] and B.X. Zhu[12]

(The Majorana Collaboration)

[1] *Nuclear Science Division, Lawrence Berkeley National Laboratory, Berkeley, CA, USA*
[2] *Pacific Northwest National Laboratory, Richland, WA, USA*
[3] *Department of Physics and Astronomy, University of South Carolina, Columbia, SC, USA*
[4] *Oak Ridge National Laboratory, Oak Ridge, TN, USA*
[5] *National Research Center "Kurchatov Institute" Institute for Theoretical and Experimental Physics, Moscow, Russia*
[6] *Joint Institute for Nuclear Research, Dubna, Russia*
[7] *Department of Physics, Duke University, Durham, NC, USA*
[8] *Triangle Universities Nuclear Laboratory, Durham, NC, USA*
[9] *Center for Experimental Nuclear Physics and Astrophysics, and Department of Physics, University of Washington, Seattle, WA, USA*
[10] *Department of Physics and Astronomy, University of North Carolina, Chapel Hill, NC, USA*
[11] *South Dakota School of Mines and Technology, Rapid City, SD, USA*
[12] *Los Alamos National Laboratory, Los Alamos, NM, USA*
[13] *Department of Physics and Astronomy, University of Tennessee, Knoxville, TN, USA*
[14] *Research Center for Nuclear Physics, Osaka University, Ibaraki, Osaka, Japan*
[15] *Department of Physics, University of South Dakota, Vermillion, SD, USA*
[16] *Department of Physics, Princeton University, Princeton, NJ, USA*
[17] *Department of Physics, North Carolina State University, Raleigh, NC, USA*
[18] *Department of Physics, Black Hills State University, Spearfish, SD, USA*
[19] *Tennessee Tech University, Cookeville, TN, USA*
[20] *Department of Physics, Engineering Physics and Astronomy, Queen's University, Kingston, ON, Canada*
[21] *Max-Planck-Institut für Physik, München, Germany*
[22] *Physik Department and Excellence Cluster Universe, Technische Universität, München, Germany*

(Dated: March 17, 2017)

We present new limits on exotic keV-scale physics based on 478 kg d of Majorana Demonstrator commissioning data. Constraints at the 90% confidence level are derived on bosonic dark matter (DM) and solar axion couplings, Pauli exclusion principle violating (PEPv) decay, and electron decay using mono-energetic peak signal-limits above our background. Our most stringent DM constraints are set for 11.8 keV mass particles, limiting g_{Ae} <4.5 $\times 10^{-13}$ for pseudoscalars and $\frac{\alpha'}{\alpha} < 9.7 \times 10^{-28}$ for vectors. We also report a 14.4 keV solar axion coupling limit of $g_{AN}^{eff} \times g_{Ae} < 3.8 \times 10^{-17}$, a $\frac{1}{2}\beta^2 < 8.5 \times 10^{-48}$ limit on the strength of PEPv electron transitions, and a lower limit on the electron lifetime of $\tau_e > 1.2 \times 10^{24}$ y for $e^- \to$ 'invisible'.

PACS numbers: 95.35.+d

The Majorana Demonstrator, described in detail in Ref. [1], is a neutrinoless double-beta decay ($0\nu\beta\beta$) experiment located 4850 ft underground at the Sanford Underground Research Facility in Lead, SD [2]. Majorana consists of two separate custom ultra-low background modules, each containing 7 arrays of P-type point contact (PPC) high-purity germanium (HPGe) detectors with a total mass of 44.1 kg, of which 29.7 kg is enriched to 88% ^{76}Ge.

The geometry of the PPC detectors results in low capacitance, reduced electronic noise, and permits good energy resolution with very low energy thresholds. In addition, PPC HPGe detectors have advantageous pulse-shape discrimination capabilities [3–5]. Previous experiments have exploited these capabilities to perform high-sensitivity searches for light WIMP and bosonic dark matter (DM) [6–8] as well as $0\nu\beta\beta$ decay searches [9–11].

In this letter, we set limits on multiple keV-scale rare-event interactions from mono-energetic signal limits with 478 kg d of Majorana commissioning data. Bosonic pseudoscalar (i.e. axion-like) and vector DM, with mass-scale of 1-100 keV, offer an explanation for the observed sub-galactic structure in the universe, assuming a large number density compensates for their light mass. With suitable electronic coupling strength, they may be detectable via a pseudoscalar or vector-electric effect that is analogous to photoelectric absorption [12–14]. In addition, we report limits on the coupling of 14.4 keV solar axions competing in the M1 transition of ^{57}Fe nuclei, Pauli Exclusion Principle violating (PEPv) electronic transitions, and electron decay, $e^- \rightarrow$ 'invisible'.

Majorana relies on careful material selection and handling [15] to reduce intrinsic and extrinsic radioactive background, making it well-suited for dark matter and other rare-event searches. Majorana modules are surrounded by a copper shield, a lead shield, an active muon veto [16], and a polyethylene neutron shield. Within the shielding, radon is purged via liquid nitrogen boil-off. The inner 5 cm of the copper shield, the cryostats that house the detectors, and the crystal support structures are fabricated from radiopure (<0.1 μBq/kg U) copper electroformed in an underground facility.

The data presented here were acquired during the June 30 to Sept. 22, 2015 commissioning of Majorana Module 1 (M1). During this time, Module 2 was under construction and not operational. The shield was incomplete: the innermost 5 cm of electroformed copper shielding was not yet installed, the active muon-veto system wasn't finished, and the exterior neutron shielding did not fully enclose the inner layers. Shielding inside and outside the vacuum and cryogenic services still had to be added. The natural (unenriched) detectors had a high cosmogenic background compared to the enriched detectors because of different handling procedures, and were only used here for systematic studies, see Fig. 1. Seven of the enriched detectors were inoperable due to failed electrical connections or high noise rates. The active mass of the remaining 13 enriched detectors was computed from detector dead layer measurements provided by ORTEC [17] and verified via collimated ^{133}Ba source scans, totaling 10.06 ± 0.13 kg. The commissioning live-time was 47.503 ± 0.001 d, resulting in an exposure of 478 ± 6 kg d.

The data-acquisition (DAQ) system is controlled and monitored by the ORCA software package [18]. Signals from the PPC detectors are amplified and shaped by a custom low-noise resistive-feedback pre-amplifier with a measured equivalent noise charge (ENC) of ~85 eV in Ge-detector-equivalent FWHM resolution [19]. The amplifier provides low-gain and high-gain outputs that are digitized separately by a custom 14-bit 100 MHz VME-based digitizer designed for the GRETINA experiment [20]. Signals are digitized continuously and triggers are generated when the output of a firmware-based trapezoidal filter trigger exceeds the pre-set threshold for that channel. An internal pulser (~0.1 Hz), implemented by injecting charge through capacitive coupling to the gate of the preamplifier's front-end JFET, is used to monitor detector live time and gain stability.

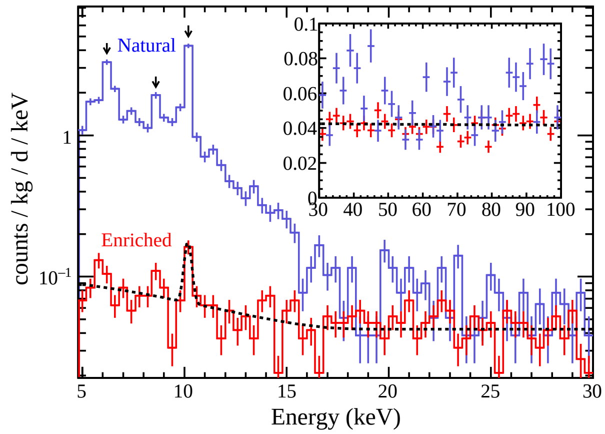

FIG. 1. (Color online) Energy spectra from 195 kg d of natural (blue) and 478 kg d of enriched (red) detector data. A fit of the background model (linear + tritium beta spectrum + ^{68}Ge K-shell) to the enriched spectrum is also shown (dotted black). The background rate and slope, along with the tritium and K-shell rate were floated in the fit. The background fit χ^2/NDF is 75.7/85. Cosmogenic isotopes in the natural detectors produce peaks at 10.36 keV (^{68}Ge), 8.9 keV (^{65}Zn), and 6.5 keV (^{55}Fe) on top of a tritium beta decay continuum. The FWHM of the 10.4 keV peak is ~0.4 keV. The spectrum shown does not include a T/E cut acceptance correction.

Transient and other irregular noise pulses from the DAQ hardware contaminate the energy-spectrum between $2-70$ keV. Most of the non-physical waveforms are due to accidental re-triggering during baseline restoration after pulser events. These are removed by eliminating events with more than one detector hit or by using pulse-shape discrimination. The acceptance of these cuts is 99.98% with negligible uncertainty.

Slow pulse waveforms with rise-times of ~1 μs or longer constitute a significant background below 30 keV, as recognized by previous experiments [6–8, 21]. Slow pulses are energy-degraded events that originate in low-field regions of the detector near the surface dead layer, where diffusion is the dominant mode of charge transport. At energies <10 keV, discriminating slow pulses using pulse rise-time measurements becomes difficult since signal to noise ratio decreases with energy.

A more robust parameter, T/E, was developed to tag slow-pulses. A trapezoidal filter with a 100 ns ramp time and a 10 ns flat-top time was applied to each waveform, and the maximum (T) value of the result was measured. The T-value was normalized by an energy parameter, (E), which was reconstructed offline by finding the maximum [22] of a trapezoidal filtered waveform with a filter rise time of 4 μs and flat-top time of 2.5 μs. This parameter exhibited good separation between fast and slow-pulse waveforms down to ~3 keV, below the 5 keV analysis threshold.

The signal acceptance of the T/E cut was measured by capacitively injecting simulated signal pulses of varying amplitude directly onto the detector's outer contact using a precision waveform generator. The energy dependent acceptance was determined by finding the fraction of these events that pass the cut at set pulse amplitudes. An error function was fit to the acceptance fractions to estimate the acceptance between pulser-peak events. Only 3 of the 13 analysis detectors were instrumented with the required electronics to perform this test and the smallest-valued (most conservative) acceptance function, ranging from 96% at 5 keV to 100% at 20 keV, was applied in the DM rate analysis, Eq 4. The detector acceptance functions varied by at most 1%. The energy dependent acceptance uncertainty was determined from the error function fit:

$$\eta(E) = \frac{\mathrm{Erf}(E-\mu)}{\sqrt{2}\sigma} \tag{1}$$

The fit values were $\mu = -26 \pm 4$ keV and $\sigma = 13.7 \pm 1.7$ keV with a strong anti-correlation, corr(μ, σ) ~ -1.

A ^{228}Th line source inserted into a helical calibration track surrounding the cryostat was used for energy calibration. Multiple calibration periods were interspersed between background data collection to track and account for long-term drift in gain. Statistically significant peaks in the ^{228}Th decay chain energy spectrum were used to calibrate the energy spectra of each detector independently. To extend our calibration to lower energies, we included the measured baseline noise as the zero point energy in the fit. For an overview of the calibration system, see [23].

We combined the calibration spectra from the 13 detectors, and summed a total of 102.8 hours of calibration data over all of the calibration periods. The resulting high statistics spectrum permitted peaks from Bi X-rays and from Th and Pb gamma rays. These were used to help quantify biases and uncertainties in the energy scale below 120 keV. A small systematic offset in the energy-scale (E_S) of ~0.2 keV from known peak energies was observed in this region. The offset is consistent with residual digitizer nonlinearity effects, which were estimated by comparing energy measurements from low-gain and high-gain channels. A linear correction (ΔE):

$$\Delta E(E_S) = \alpha_E(E_S - 95.0\,\mathrm{keV}) + E_0\ , \tag{2}$$

was applied to mitigate the offset. The parameters $\alpha_E = -0.0014 \pm 0.0008$ and $E_0 = -0.256 \pm 0.016$ keV were determined by fitting a line to the peak-centroid offset values of the low-statistics peaks between 70 and 120 keV. The correlation coefficient was $\mathrm{corr}(\alpha_E, E_0) = -0.22$. The correction was then extrapolated to lower energies. As a check, the predicted offset at 10.36 keV, the ^{68}Ge cosmogenic K-shell cascade peak, was computed and found to be -0.12 ± 0.07 keV. In the natural detectors, this peak was measured at 10.22 keV, and is consistent with the correction model prediction in Eq. 2 to within the parameter uncertainties. We are improving our nonlinearity correction and expect to remove this offset in future analyses.

A multi-peak fitting routine was applied to the summed ^{228}Th calibration spectrum to determine the energy-dependent widths (σ) of peaks in the 1-260 keV energy range. The widths were fit to:

$$\sigma_E(E) = \sqrt{\sigma_0^2 + \langle\varepsilon\rangle F E}\ , \tag{3}$$

with resulting fit values of $\sigma_0 = 0.16 \pm 0.04$ keV and $F = 0.11 \pm 0.02$. The fit parameters were fully correlated, $\mathrm{corr}(\sigma_0, F) \sim 1$. The constant $\langle\varepsilon\rangle = 2.96$ eV, is the average energy required to produce an electron-hole pair in Ge.

Limits on pseudoscalar dark matter axio-electric coupling were calculated using a method similar to [24]. For comparison with other experiments, we set the Milky Way halo density to $\rho_{DM} = 0.3$ GeV cm^{-3} [25] and assumed that pseudoscalar DM constitutes the total density. The expected number of detected counts, dN/dE at energy E, assuming a pseudoscalar mass of m_A in keV, is given by [24, 26],

$$\frac{dN}{dE}(E; m_A) = \Phi_{DM}(m_A)\sigma_{Ae}(m_A) \\ \eta(E)\frac{1}{\sqrt{2\pi}\sigma_E(m_A)}\exp\left(-\frac{(E-m_A)^2}{2\sigma_E^2(m_A)}\right) MT\ , \tag{4}$$

$$\Phi_{DM} = \rho_{DM}\frac{v_A}{m_A} = 7.8 \times 10^{-4}\left(\frac{1}{m_A}\right)\cdot\beta\ [\text{/barn/day}], \tag{5}$$

$$\sigma_{Ae}(m_A) = \sigma_{pe}(m_A)\frac{g_{Ae}^2}{\beta}\frac{3m_A^2}{16\pi\alpha m_e^2}\left(1 - \frac{\beta^{\frac{2}{3}}}{3}\right). \tag{6}$$

where $\beta = v_A/c$ is the average DM velocity with respect to the earth, Φ_{DM} is the average DM flux at Earth, σ_{Ae} is the axio-electric cross section as a function of energy, σ_E is the energy resolution at $E = m_A$ (given by Eq. 3), MT is the exposure of the detectors used in this analysis, and $\eta(E)$ is the T/E cut acceptance function (Eq. 1). In Eq. 6, σ_{pe} is the photoelectric cross section in Ge [27]. In this analysis, the peak energy of interest is the pseudoscalar mass (m_A). We take $\beta = 0.001$ [24, 28], roughly the mean of the dark matter velocity distribution with respect to the Earth.

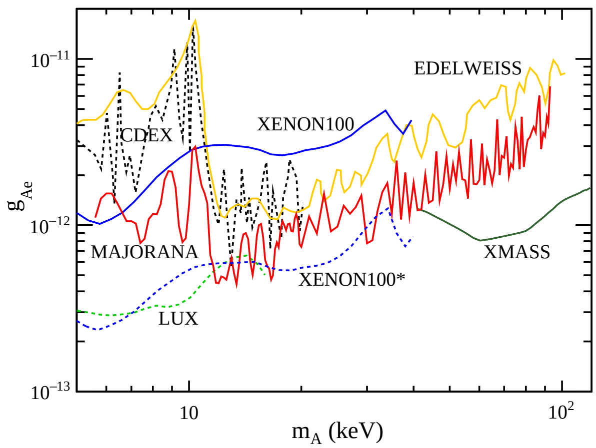

FIG. 2. (Color online) The 90% UL on the pseudoscalar axion-like particle dark mater coupling from the Majorana Demonstrator (red) compared to EDELWEISS [24] (orange), XMASS [33] (dark green), and XENON [28] (blue). XENON has recently published an erratum [34] (dashed blue). Results by LUX (dashed, light green) have not yet been published [35], and new results from CDEX [32] (dashed, black) are available on the arXiv [32].

We place an upper limit on the pseudoscalar dark matter coupling constant, g_{Ae}, at multiple m_A values between 5-100 keV using an unbinned profile likelihood method [29–31]. The likelihood function incorporates a DM signal PDF that is modeled separately with Eq. 4 for each individual m_A value, a linear background, the tritium spectrum and a 10.36 keV cosmogenic x-ray peak. A multi-dimensional Gaussian penalty term floats the nuisance parameters (α_E, E_0, σ_E, and η) in the likelihood function according to their covariance matrices. The penalty term affects the final limit by a few percent at most. The best fit to the background model is shown in Fig. 1.

A comparison of our g_{Ae}-limits, as a function of pseudoscalar mass, to previous results is shown in Fig. 2. Our limits are an improvement over other germanium experiments, EDELWEISS [24] and CDEX [32], especially for $m_A < 18.6$ keV due to the low cosmogenic activity in Majorana enriched detectors. The XMASS [33] experiment has the best limits for $m_A > 40$ keV. Two XENON limits are shown: the original published in [28] (solid), and a correction from an erratum [34] (dashed). Preliminary LUX results [35] are comparable to the revised XENON results. Currently the xenon experiments: XMASS, XENON, and LUX report the best limits due to the >10× larger exposure of their fiducial mass.

Using the same data and analysis technique with a gaussian modeled signal, we also set limits on the electronic coupling of vector bosonic DM [12]. The interaction rate for vector DM is:

$$\Phi_{DM}(m_V)\sigma_{Ve}(m_V) = \frac{4\times10^{23}}{m_V}\left(\frac{\alpha'}{\alpha}\right)\frac{\sigma_{pe}(m_V)}{A}\ [/\mathrm{kg/d}], \tag{7}$$

where A is the atomic mass of Ge, m_V is the vector boson mass in keV, and α' is the coupling of vector DM to electrons, analogous to the electromagnetic fine structure constant, α. The expected number of detector counts at energy E is found by replacing the axio-electric interaction rate in Eq. 4 with the vector-electric rate, with m_V substituted for m_A. Limits on the vector coupling from the unbinned likelihood analysis described above are shown in Fig. 3. In the case of vector DM, the experimental constraints are more stringent than astrophysical limits, excepting red giant (RG) stars.

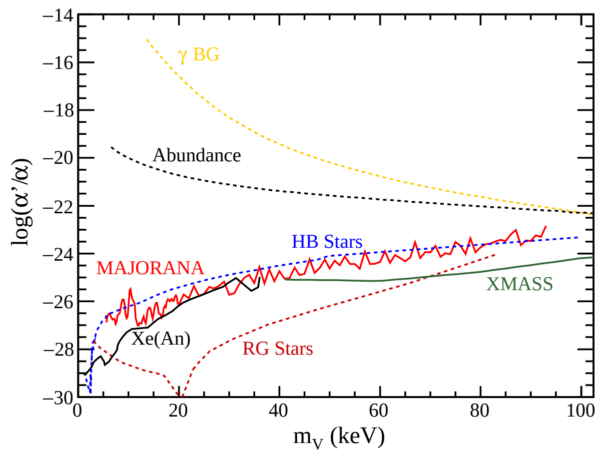

FIG. 3. (Color online) The 90% UL on the vector particle dark mater coupling from the Majorana Demonstrator (red) compared to the astrophysical limits (dashed) from the gamma background (orange), the observed dark matter abundance (black), HB stars (blue), and RG stars (maroon) [12, 36]. Experimental results (solid) from XMASS [33] (green) along with a 2σ limit computed from XENON100 [28] data by H. An, et al. [37] are also shown.

In addition to generic pseudoscalar and vector DM, we analyzed our sensitivity to solar axions. ^{57}Fe has a large solar abundance and its first excited state at 14.4 keV is thermally excited within the Sun's interior. Axion emission is possible from the decay of this state [38]. Electric coupling of these axions to atomic electrons in the detector would manifest as a peak at 14.4 keV. No such peak was observed in Majorana, and a limit on the product of the effective axio-nuclear coupling, g_{AN}^{eff}, of solar axions (see [39]) and the axio-electric coupling, g_{Ae}, was determined. Replacing the flux in Eq. 5 with [24]

$$\Phi_{14.4} = \beta^3 \times 4.56\times10^{23}(g_{AN}^{eff})^2\ [/\mathrm{cm}^2/\mathrm{s}], \tag{8}$$

and substituting m_A in Eq. 4 with 14.4 keV, we use the unbinned likelihood analysis to determine a limit on the coupling constant. Since this is a mono-energetic transition, the reduced axion velocity, β, depends on the mass of the axion, which can range from zero to 14.4 keV. In the low mass limit where $\beta \to 1$, we find a 90% UL of $g_{AN}^{eff} \times g_{Ae} < 3.8 \times 10^{-17}$. A comparison of the MAJORANA and EDELWEISS coupling limits is shown in Fig. 4.

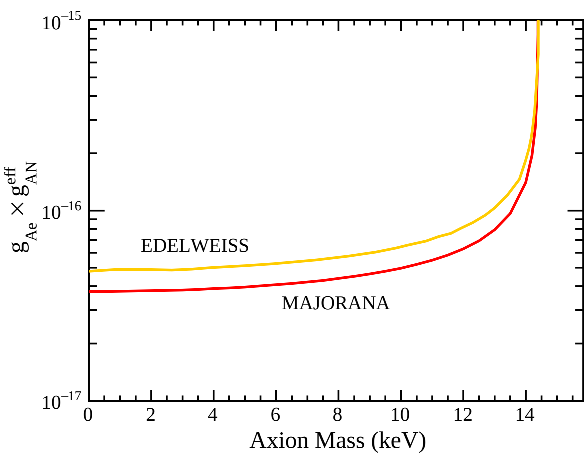

FIG. 4. (Color online) The 90% UL coupling of 14.4-keV solar axions from the MAJORANA DEMONSTRATOR (red) data compared with the limit set by EDELWEISS (orange). The product of the axio-nuclear coupling in the sun and the axio-electric coupling in the detector is shown. Comparative astrophysical limits assuming g_{AN}^{eff} follows the DFSZ model is shown in Ref. [24].

Two other non-DM related rare-event searches were carried out using the low energy data and analysis, a Pauli Exclusion violating decay and an electron decay search. While the Pauli Exclusion Principle is a fundamental law of nature, its physical origin is still not fully understood [40–45]. MAJORANA searched for the PEPv transition of an L-shell Ge electron to the K-shell that would manifest as a 10.6 keV [44] shoulder on the 10.36 keV ^{68}Ge peak. Using the unbinned likelihood method with a generic signal plus background model, we set a 90% CL on the excess signal rate of 0.03 /kg/d. This equates to a lifetime $\tau > 2.0 \times 10^{31}$ s. Comparing to the 1.7×10^{-16} s lifetime of a standard K_α transition in Ge, one derives an upper limit on the PEPv parameter $\frac{1}{2}\hat{\beta}^2 < 8.5 \times 10^{-48}$, a ∼35% improvement over the previous limit [46].

Our data can also be used to set a limit on the decay of the electron. Charge conservation arises from an exact gauge symmetry of quantum electrodynamics with the associated gauge boson being exactly massless. Even so, the possibility of its violation has been theoretically explored [47–53]. For example, the charge-conservation violating process $e^- \to \nu\bar{\nu}\nu$ would produce an atomic-shell hole. If an electron disappears from the K shell of a Ge atom, resulting atomic emissions will deposit 11.1 keV of energy within the detector. We search for events of this characteristic energy as possible indications of electron decay using a similar analysis as for the PEPv and solar axion search. We determined a lifetime limit of $>1.2\times10^{24}$ y. The best limit on the lifetime for this process is $>2.4\times10^{24}$ y (90% CL) [54].

We found no indication of new physics that would manifest as a peak in the energy-spectrum of the Module 1 commissioning data presented in this paper. Upgrades to MAJORANA, detector repairs, and the addition of Module 2, will significantly improve the sensitivity to new physics. Lower background rates in subsequent data sets have already been observed with the installation of the inner electroformed-copper and additional polyethylene neutron shielding. Analysis thresholds below 5 keV will allow us to constrain additional processes including light-WIMP scattering.

This material is based upon work supported by the U.S. Department of Energy, Office of Science, Office of Nuclear Physics under Award Numbers DE-AC02-05CH11231, DE-AC52-06NA25396, DE-FG02-97ER41041, DE-FG02-97ER41033, DE-FG02-97ER41042, DE-SC0012612, DE-FG02-10ER41715, DE-SC0010254, and DE-FG02-97ER41020. We acknowledge support from the Particle Astrophysics Program and Nuclear Physics Program of the National Science Foundation through grant numbers PHY-0919270, PHY-1003940, 0855314, PHY-1202950, MRI 0923142 and 1003399. We acknowledge support from the Russian Foundation for Basic Research, grant No. 15-02-02919. We acknowledge the support of the U.S. Department of Energy through the LANL/LDRD Program. This research used resources of the Oak Ridge Leadership Computing Facility, which is a DOE Office of Science User Facility supported under Contract DE-AC05-00OR22725. This research used resources of the National Energy Research Scientific Computing Center, a DOE Office of Science User Facility supported under Contract No. DE-AC02-05CH11231. We thank our hosts and colleagues at the Sanford Underground Research Facility for their support.

---

* Alternate address: Department of Nuclear Engineering, University of California, Berkeley, CA, USA
† Corresponding author. Email: krisvorren@unc.edu

[1] N. Abgrall *et al.*, Advances in High Energy Physics, **2014**, 1 (2014).
[2] J. Heise, J. Phys. Conf. Ser., **606**, 1 (2015), arXiv:1503.01112.
[3] P. Luke *et al.*, IEEE Trans. on Nucl. Sci., **36**, 926 (1989).
[4] P. S. Barbeau, J. I. Collar, and O. Tench, JCAP, **09**, 009 (2007).
[5] R. Cooper *et al.*, Nucl. Instrum. Meth. A, **629**, 303 (2011), ISSN 0168-9002.
[6] G. Giovanetti *et al.*, Phys. Proc., **61**, 77 (2015), ISSN

1875-3892.

[7] C. E. Aalseth *et al.*, (2014), arXiv:1401.3295.

[8] W. Zhao *et al.*, Phys. Rev. D, **88**, 052004 (2013), arXiv:1306.4135.

[9] H. V. Klapdor-Kleingrothaus, A. Dietz, H. L. Harney, and I. V. Krivosheina, Mod. Phys. Lett., **A16**, 2409 (2001), arXiv:hep-ph/0201231 [hep-ph].

[10] C. E. Aalseth *et al.*, Phys. Rev. D, **65**, 092007 (2002).

[11] K.-H. Ackermann *et al.*, The European Physical Journal C, **73**, 2330 (2013), ISSN 1434-6052.

[12] M. Pospelov, A. Ritz, and M. Voloshin, Phys. Rev. D, **78**, 115012 (2008).

[13] J. Redondo and M. Postma, J. Cosm. Astropart. Phys., **2**, 5 (2009).

[14] H. An, M. Pospelov, J. Pradler, and A. Ritz, Phys. Lett. B, **747**, 331 (2015).

[15] N. Abgrall *et al.*, Nucl. Instrum. Meth. A, **828**, 22 (2016).

[16] N. Abgrall *et al.* (Majorana), (2016), arXiv:1602.07742 [nucl-ex].

[17] ORTEC, 801 South Illinois Avenue Oak Ridge, TN 37830, USA.

[18] M. A. Howe *et al.*, IEEE Trans. Nucl. Sci., **51**, 878 (2004).

[19] P. Barton, P. Luke, M. Amman, Y.-D. Chan, J. Detwiler, J. Loach, R. Martin, A. Poon, C. Tindall, and K. Vetter, in *Proceedings, 2011 IEEE Nuclear Science Symposium and Medical Imaging Conference (NSS/MIC 2011): Valencia, Spain, October 23-29, 2011* (2011) pp. 1976–1979.

[20] S. Paschalis *et al.*, Nucl. Instrum. Meth. A, **709**, 44 (2013), ISSN 0168-9002.

[21] E. Aguayo *et al.*, Nucl. Instrum. Meth. A, **701**, 176 (2013).

[22] Except for use in the T/E parameter, the actual calculated energy is the filtered value at a fixed time of 6 μs after the start of the rising edge, identified using a second trapezoidal filter with a 1 μs ramp time and $\sim$1 keV threshold. The energy scale is also subject to a digitizer non-linearity correction.

[23] N. Abgrall *et al.*, (2017), arXiv:1702.02466 [physics.ins-det].

[24] E. Armengaud *et al.*, JCAP, **11**, 067 (2013).

[25] Recent results suggest that the local density is closer to 0.4 GeV cm^{-3}. See Ref. [55].

[26] F. Alessandria *et al.*, JCAP, **05**, 007 (2013), arXiv:1209.2800.

[27] "NIST Physical Meas. Laboratory," `http://physics.nist.gov/PhysRefData/Xcom/html/xcom1.html` (2016), last checked 3/14/16.

[28] E. Aprile *et al.*, Phys. Rev. D, **90**, 062009 (2014).

[29] S. S. Wilks, Ann. Math. Statist., **9**, 60 (1938).

[30] W. A. Rolke, A. M. López, and J. Conrad, Nuclear Instruments and Methods in Physics Research A, **551**, 493 (2005).

[31] F. James, *Statistical Methods in Experimental Physics* (World Scientific Publishing, 2006) ISBN 9789812705273.

[32] S. K. Liu *et al.*, (2016), arXiv:1610.07521 [hep-ex].

[33] K. Abe *et al.*, Phys. Rev. Lett., **113**, 121301 (2014).

[34] E. Aprile *et al.*, Phys. Rev. D, **95**, 029904 (2017).

[35] "IDM2016 Identification of Dark Matter 2016," `https://idm2016.shef.ac.uk/` (2016), last checked 10/10/16.

[36] R. Essig *et al.*, in *Proceedings, Community Summer Study 2013: Snowmass on the Mississippi (CSS2013): Minneapolis, MN, USA, July 29-August 6, 2013* (2013) arXiv:1311.0029 [hep-ph].

[37] H. An, M. Pospelov, J. Pradler, and A. Ritz, Physics Letters B, **747**, 331 (2015), ISSN 0370-2693.

[38] S. Moriyama, Phys. Rev. Lett., **75**, 3222 (1995).

[39] S. Andriamonje *et al.*, JCAP, **12**, 002 (2009).

[40] A. Y. Ignatiev and V. A. Kuzmin, Sov. J. Nucl. Phys., **461**, 786 (1987).

[41] O. W. Greenberg and R. N. Mohapatra, Phys. Rev. Lett., **59**, 2507 (1987).

[42] O. W. Greenberg, Phys. Rev. D, **43**, 4111 (1991).

[43] O. W. Greenberg, AIP Conf. Proc., **545**, 113 (2000).

[44] S. R. Elliott *et al.*, Found. Phys., **42**, 1015 (2012), ISSN 1572-9516.

[45] N. Abgrall *et al.*, The European Physical Journal C, **76**, 619 (2016), ISSN 1434-6052.

[46] R. Bernabei *et al.*, Eur. Phys. J. C, **62**, 327 (2009), ISSN 1434-6052.

[47] L. B. Okun and Y. B. Zeldovich, Phys. Lett. B, **78**, 597 (1978).

[48] M. B. Voloshin and L. B. Okun, JETP Lett., **28**, 145 (1978).

[49] A. Ignatiev, V. Kuzmin, and Shaposhnikov, Phys. Lett. B, **84**, 315 (1978).

[50] R. Mohapatra, Phys. Rev. Lett., **59**, 1510 (1987).

[51] L. Okun, Sov. Phys. Usp., **32**, 543 (1989).

[52] R. Mohapatra and S. Nussinov, Int. J. Mod. Phys. A, **7**, 3817 (1992).

[53] A. Y. Ignatiev and G. Joshi, Phys Lett B, **381**, 216 (1996).

[54] P. Belli *et al.*, Phys. Lett. B, **460**, 236 (1999).

[55] D. Hooper, Submitted to: JCAP (2016), arXiv:1608.00003 [astro-ph.HE].